

Deep Reinforcement Learning Based Dynamic Trajectory Control for UAV-assisted Mobile Edge Computing

Liang Wang, Kezhi Wang, Cunhua Pan, Wei Xu, Nauman Aslam and Arumugam Nallanathan, *Fellow, IEEE*

Abstract

In this paper, we consider a platform of flying mobile edge computing (F-MEC), where unmanned aerial vehicles (UAVs) serve as equipment providing computation resource, and they enable task offloading from user equipment (UE). We aim to minimize energy consumption of all the UEs via optimizing the user association, resource allocation and the trajectory of UAVs. To this end, we first propose a Convex optimization based Trajectory control algorithm (CAT), which solves the problem in an iterative way by using block coordinate descent (BCD) method. Then, to make the real-time decision while taking into account the dynamics of the environment (i.e., UAV may take off from different locations), we propose a deep Reinforcement leArning based Trajectory control algorithm (RAT). In RAT, we apply the Prioritized Experience Replay (PER) to improve the convergence of the training procedure. Different from the convex optimization based algorithm which may be susceptible to the initial points and requires iterations, RAT can be adapted to any taking off points of the UAVs and can obtain the solution more rapidly than CAT once training process has been completed. Simulation results show that the proposed CAT and RAT achieve the similar performance and both outperform traditional algorithms.

Index Terms

Deep Reinforcement Learning, Mobile Edge Computing, Unmanned Aerial Vehicle (UAV), Trajectory Control, User Association

Liang, Kezhi and Nauman are with the Department of Computer and Informantion Science, Northumbria University, Newcastle upon Tyne, UK, NE1 8ST. Cunhua and Arumugam are with School of Electronic Engineering and Computer Science, Queen Mary University of London, E1 4NS, U.K. Wei is with National Mobile Communications Research Lab, Southeast University, China.

I. INTRODUCTION

With the popularity of computationally-intensive tasks, e.g., smart navigation and augmented reality, people are expecting to enjoy more convenient life than ever before. However, current smart devices and user equipments (UEs), due to small size and limited resource, e.g., computation and battery, may not be able to provide satisfactory Quality of Service (QoS) and Quality of Experience (QoE) in executing those highly demanding tasks.

Mobile edge computing (MEC) has been proposed by moving the computation resource to the network edge and it has been proved to greatly enhance UE's ability in executing computation-hungry tasks [1]. Recently, flying mobile edge computing (F-MEC) has been proposed, which goes one step further by considering that the computing resource can be carried by unmanned aerial vehicles (UAVs) [2]. F-MEC inherits the merits of UAV and it is expected to provide more flexible, easier and faster computing service than traditional fixed-location MEC infrastructures. However, the F-MEC also brings several challenges: 1) how to minimize the long-term energy consumption of all UEs by choosing proper user association (i.e., whether UE should offload the tasks and if so, which UAV to offload to, in the case of multiple flying UAVs); 2) how much computations the UAV should allocate to each offloaded UE by considering the limited amount of on-board resource; 3) how to control each UAV's trajectory in real time (namely, flying direction and distance), especially considering the dynamic environment (i.e., the UAV may take off from different starting points). Traditional approaches like exhaustive search are hardly to tackle the above problems due to the fact that the decision variable space of F-MEC, e.g., deciding the optimal trajectory and resource allocation, is continuous instead of discrete. In [3], the authors propose a quantized dynamic programming algorithm to address the resource allocation problem of MEC. However, the complexity of this approach is very high as the flying choice of UAV is nearly infinite (as continuous variables). Moreover, the authors in [4] discretize the UAV trajectory into a sequence of UAV locations and make their proposed problem tractable. Similarly, in [5], the authors assume that the UAV's trajectory can be approximated by using the discrete variables and then they deal with it by using the traditional convex optimization approaches. However, the above treatment may decrease the control accuracy of the UAV and also is not flexible. Furthermore, the above contributions only considered a single UAV case. In practice, one UAV may not have enough resource to serve all the users. If the served area is very large, more than one UAV are normally needed, which will undoubtedly increase the decision space and make

it very difficult for the traditional convex optimization based approaches to obtain the optimal control strategies of each UAV. In [6], Liu *et al.* propose a deep reinforcement learning based DRL-EC³ algorithm, which can control the trajectory of multiple UAVs but did not consider the user association and resource allocation.

Inspired by the challenges mentioned above, in this paper, we first propose a Convex optimization based Trajectory control algorithm (CAT) to minimize the energy consumption of all the UEs, by jointly optimizing user association, resource allocation and UAV trajectory. Specifically, by applying block coordinate descent (BCD) method, CAT is divided into two parts, i.e., subproblems for deciding UAV trajectories and for deciding user association and resource allocation. In each iteration, we solve each part separately while keep the other part fixed, until the convergence is achieved.

Next, we propose a deep Reinforcement leArning based Trajectory control algorithm (RAT) to facilitate the real-time decision making. In RAT, two deep Q networks (DQNs), i.e., actor and critic networks are applied, where the actor network is responsible for deciding the direction and flying distance of the UAV, while the critic network is in charge of evaluating the actions generated by the actor network. Then, we propose a low-complexity matching algorithm to decide the user association and resource allocation with the UAVs. We choose the overall energy consumption of all the UEs as a reward of the RAT. In addition, we deploy a mini-batch to collect samples from the experience replay buffer by using a Prioritized Experience Replay (PER) scheme.

Different from the traditional optimization based algorithms which normally need iterations and are susceptible to the initial points, the proposed RAT can be adapted to any taking off points of the UAVs and can obtain the solutions very rapidly once the training process has been completed. In other words, if the starting off points of the UAV are input to the RAT, the trajectories of the UAVs will be determined by the proposed RAT with only some simple algebraic calculations instead of solving the original optimization problem through traditional high-complexity optimization algorithms. This attributes to the fact that during the training stages, excessive randomly taking off points of UAV are generated and used to train the networks until the networks are converged. Also, with the help of prioritized experience reply (PER), the convergence speed will be increased significantly. RAT can be applied to the practical scenarios where the UAVs needs to act and fly swiftly such as the battlefields. By inputting the current coordinates as the starting off points to the networks, the trajectories of the UAVs will be

immediately obtained and then all the UAVs can take off and fly according to the obtained trajectories. Also, the resource allocation and user association are determined by the proposed low-complexity matching algorithm. This is particularly useful to some emergence scenarios (e.g., battlefields, earthquake, large fires), as fast decision making is crucial in these areas.

In the simulation, we can see that the proposed RAT can achieve the similar performance as the convex-based solution CAT. They both have considerable performance gain over other traditional algorithms. In addition, we can see that during the learning procedure, the proposed RAT is less sensitive to the hyperparameters, i.e., the size of mini-batch and the experience replay buffer, when comparing to traditional reinforcement learning where PER is not applied.

The remainder of this paper is organized as follows. Section II presents the related work. Section III describes the system model. Section IV introduces the proposed CAT algorithm, whereas Section V gives the proposed RAT algorithm including the preliminaries of DRL. The simulation results are reported in Section VI. Finally, conclusions are given in Section VII.

II. RELATED WORK

There are many related works that study UAV, MEC and DRL separately, but only a very few consider them holistically. For UAV aided wireless communications, several scenarios have been studied, such as in areas of relay transmissions [7]–[9], cellular system [10], data collection [11]–[14], wireless power transfer [15], caching networks [16], and D2D communication [17]. In [18], the authors presented an approach to optimize the altitude of UAV to guarantee the maximum radio coverage on the ground. In [19], the authors presented a fly-hover-and-communicate protocol in a UAV-enabled multiuser communication system. They partitioned the ground terminals into disjoint clusters and deployed the UAV as a flying base station. Then, by jointly optimizing the UAV altitude and antenna beamwidth, they optimized the throughput in UAV-enabled downlink multicasting, downlink broadcasting, and uplink multiple access models. In [4], to maximize the minimum average throughput of covered users in OFDMA system, the authors proposed an efficient iterative algorithm based on block coordinate descent and convex optimization techniques to optimize the UAV trajectory and resource allocation. Furthermore, UAV trajectory optimization research were also investigated. For instance in [20], Zeng *et al.* proposed an efficient design by optimizing UAV's flight radius and speed for the sake of maximizing the energy efficiency of UAV communication. In order to maximize the minimum throughput of all mobile terminals in cellular networks, Lyu *et al.* [13] developed a new hybrid network architecture

by deploying UAV as an aerial mobile base station. Different from [4], [18]–[20] with the single UAV system, a multi-UAV enabled wireless communication system was considered to serve a group of users in [21]. Also, in [22], resource allocation between communication and computation has been investigated in multi-UAV systems.

In addition, some recent literature made efforts to mobile edge computing (MEC), which is considered to be a promising technology for bringing computing resource to the edge of the wireless networks [23], where UEs can benefit from offloading their intensive tasks to MEC servers. In [24], partial computation offloading was studied. The computation tasks can be divided into two parts, where one part is executed locally and the other part is offloaded to MEC servers. In [25], binary computation offloading was studied, where the computation tasks can either be executed locally or offloaded to MEC servers.

By taking the advantage of the mobility of UAVs, UAV-enabled MEC has also been studied in [26], [27]. In [26], the authors minimized the overall mobile energy consumption by jointly optimizing UAV trajectory and bit allocation, while satisfying QoS requirements of the offloaded mobile application. In [27], the authors studied UAV-enabled MEC, where wireless power transfer technology is applied to power the Internet of things devices and collect data from them.

For most of the above works, optimization theory are mainly applied in order to obtain the optimal and / or suboptimal solutions, e.g., trajectory design and resource allocation. However, solving such optimization problems normally requires plenty of computational resources and take much time. To address this problem, DRL has been applied and attracted much attention recently. In [28], the authors proposed a RL framework that uses DQN as the function approximator. In addition, two important ingredients experience replay and target network are used for improving the convergence performance. In [29], the authors pointed out that the classical DQN algorithm may suffer from substantial overestimations in some scenarios, and proposed a double Q-learning algorithm. In order to solve control problems with continuous state and action space, Lillicrap *at al.* [30] proposed a policy gradient based algorithm. For the purpose of obtaining faster learning and state-of-art performance, in [31], the authors proposed a more robust and scalable approach named prioritized experience replay. Although DRL has achieved remarkable successes in game-playing scenarios, it is still an open research area in UAV-enabled MEC.

III. SYSTEM MODEL

As shown in Fig. 1, we consider a scenario that there are N UEs with the set denoted as $\mathcal{N} = \{1, 2, \dots, N\}$ and M UAVs with the set denoted as $\mathcal{M} = \{1, 2, \dots, M\}$, which form an F-MEC platform. To make it clear, the main notations used in this paper are listed in Table. I.

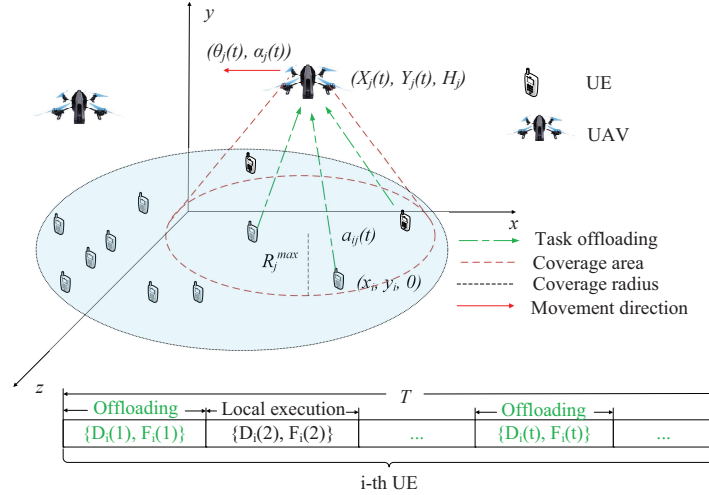


Fig. 1: Multi-UAV enabled F-MEC architecture.

We assume that the i -th UE constantly generates one task $I_i(t)$ in the t -th time slot and lasting for T time slots. Then, T tasks will be generated for each UE and one has $t \in \mathcal{T} = \{1, 2, \dots, T\}$ and

$$I_i(t) = \{D_i(t), F_i(t)\}, \forall i \in \mathcal{N}, t \in \mathcal{T}, \quad (1)$$

where $D_i(t)$ denotes the size of data required to be transmitted to a UAV if the UE chooses to offload the task, and $F_i(t)$ denotes the total number of CPU cycles needed to execute this task. Assume that each UE can choose either to offload the task to one of the UAVs or execute the task locally. Then one can have

$$a_{ij}(t) = \{0, 1\}, \forall i \in \mathcal{N}, j \in \mathcal{M}, t \in \mathcal{T}, \quad (2)$$

where $a_{ij}(t) = 1, j \neq 0$ implies that the i -th UE decides to offload the task to the j -th UAV in the t -th time slot, while $a_{ij}(t) = 1, j = 0$ means that the i -th UE executes the task itself in the t -th time slot, and otherwise, $a_{ij}(t) = 0$. Define a new set $j \in \mathcal{M}' = \{0, 1, 2, \dots, M\}$ to represent the possible place where the tasks from UEs can be executed, where $j = 0$ indicates that UE conducts its own task locally without offloading.

TABLE I: Main Notations.

Notation	Definition
i, N, \mathcal{N}	Index of an UE, the number of UAVs and the set of of UEs, respectively
$j, M, \mathcal{M}, \mathcal{M}'$	Index of an UAV, the number of UAVs, the set of UAVs and the set of offloading places, respectively
t, T, \mathcal{T}	Index of a timeslot, the number of timeslots and the set of timeslots, respectively
$I_i(t)$	The i -th UEs' task in t -th time slot
$D_i(t)$	The data size of i -th UEs' task in t -th time slot
$F_i(t)$	The required CPU cycles of i -th UEs' task in t -th time slot
$a_{ij}(t)$	User association between i -th UE and j -th place in t -th timeslot
R_j^{\max}	Maximal horizontal coverage range of j -th UAV
$\theta_j(t), d_j(t)$	Flying direction and flying distance of j -th UAV, respectively
d_j^{\max}, v_j	Maximal flying distance and flying velocity of j -th UAV, respectively
$[X_j(t), Y_j(t), H_j]$	Coordinates of j -th UAV in t -th timeslot
T^{\max}	Maximal duration of timeslot
$V_j^{\max}, f_j^{\max}(t)$	Maximal number of tasks and maximal computation resource that j -th UAV possesses, respectively
$[x_i, y_i]$	Coordinates of i -th UE
$R_{ij}(t)$	Euclidean distance between i -th UE and j -th UAV in t -th timeslot
$B, P_i^{\text{Tr}}, g_0, \sigma^2$	Channel bandwidth, transmitting power, channel power gain and noise power, respectively
$T_{ij}^{\text{O}}(t), T_{ij}^{\text{Tr}}(t), T_{ij}^{\text{C}}(t)$	The time for task completion and offloading, and executing, respectively
$E_{ij}^{\text{Tr}}(t), E_{ij}^{\text{L}}(t)$	Energy consumption for offloading and local execution, respectively
$\mathbf{U}, \mathbf{G}, \mathbf{A}, \mathbf{F}$	The set of UAV trajectory, UAV coordinates, user association and resource allocation, respectively
$s(t), a(t), z(t)$	State, action and reward in t -th timeslot, respectively
$\lambda_j(t), \alpha_j(t)$	Factor of flying direction and flying distance in t -th timeslot, respectively
$\pi(\cdot), Q(\cdot), L(\cdot)$	Policy function, Q function and loss function, respectively
ϕ, δ, J	Network parameter, TD-error and policy gradient, respectively

In addition, we assume that each UE can only be served by at most one UAV or itself, and each task only has one place to execute. Then, it follows

$$\sum_{j=0}^M a_{ij}(t) = 1, \forall i \in \mathcal{N}, t \in \mathcal{T}. \quad (3)$$

A. UAV Movement

Assume that the j -th UAV flies at a fixed altitude H_j like [19], and it has a maximal horizontal coverage R_j^{\max} , which depends on the transmitting angle of antennas and the flying altitude. Also, assume that in the t -th time slot, the j -th UAV can fly with direction as

$$0 \leq \theta_j(t) \leq 2\pi, \forall j \in \mathcal{M}, t \in \mathcal{T}, \quad (4)$$

and distance as

$$0 \leq d_j(t) \leq d_j^{\max}, \forall j \in \mathcal{M}, t \in \mathcal{T}, \quad (5)$$

where one can have the maximal flying distance in each time slot as $d_j^{\max} = v_j T^{\max}$, v_j is the constant flying velocity, T^{\max} is the maximal duration of the time slot. We also denote the coordinate of the j -th UAV in the t -th time slot as $[X_j(t), Y_j(t), H_j]$, where $X_j(t) = X_j(0) + \sum_{l=1}^t d_j(l) \cos \theta_j(l)$, $Y_j(t) = Y_j(0) + \sum_{l=1}^t d_j(l) \sin \theta_j(l)$ and $[X_j(0), Y_j(0), H_j]$ is the starting coordinate of the j -th UAV. Then, the flying time of the j -th UAV in the t -th time slot is

$$T_j^{\text{uav}}(t) = \frac{d_j(t)}{v_j}, \forall j \in \mathcal{M}, t \in \mathcal{T}, \quad (6)$$

and one has

$$T_j^{\text{uav}}(t) \leq T^{\max}, \forall i \in \mathcal{N}, j \in \mathcal{M}. \quad (7)$$

Also, in each time slot, we assume that each UAV can accept the limited amount of offloaded tasks. Then, one has

$$\sum_{i=1}^N a_{ij}(t) \leq V_j^{\max}, \forall j \in \mathcal{M}, t \in \mathcal{T}, \quad (8)$$

where V_j^{\max} is the maximal number of tasks that the j -th UAV can accept in the t -th time slot.

B. Task Execution

If the i -th UE decides to offload the task to the j -th UAV in the t -th time slot, then the euclidean distance $R_{ij}(t)$ can be written as

$$R_{ij}(t) = \sqrt{(X_j(t) - x_i)^2 + (Y_j(t) - y_i)^2}, \quad (9)$$

where $[x_i, y_i]$ is the coordinate of the i -th UE, and it has

$$a_{ij}(t) R_{ij}(t) \leq R_j^{\max}, \forall i \in \mathcal{N}, j \in \mathcal{M}, t \in \mathcal{T}. \quad (10)$$

where R_j^{\max} is the maximal horizontal coverage of the j -th UAV. Then, the uplink data rate is given by

$$r_{ij}(t) = B \log_2 \left(1 + \frac{\alpha P_i^{\text{Tr}}}{H_j^2 + R_{ij}^2(t)} \right), \forall i \in \mathcal{N}, j \in \mathcal{M}, t \in \mathcal{T}, \quad (11)$$

where B is the bandwidth for each communication channel; P_i^{Tr} is the transmitting power of the i -th UE; $\alpha = \frac{g_0 G_0}{\sigma^2}$ with $G_0 \approx 2.2846$; g_0 is the channel power gain at the reference distance 1 m and σ^2 is the noise power. Note that we consider each user applies orthogonal frequency division multiplexing (OFDM) channel and there is no interference among them.

If the i -th UE decides to offload its task to the j -th UAV in the t -th time slot, the total task completion time is given by

$$T_{ij}^O(t) = T_{ij}^{\text{Tr}}(t) + T_{ij}^{\text{C}}(t), \quad t \in \mathcal{T}, \quad (12)$$

where $T_{ij}^{\text{Tr}}(t)$ is the time to offload the data from the i -th UE to the j -th UAV in the t -th time slot, given by

$$T_{ij}^{\text{Tr}}(t) = \frac{D_i(t)}{r_{ij}(t)}, \quad t \in \mathcal{T}, \quad (13)$$

and $T_{ij}^{\text{C}}(t)$ is the time required to execute the task at the UAV as

$$T_{ij}^{\text{C}}(t) = \frac{F_i(t)}{f_{ij}^{\text{C}}(t)}, \quad t \in \mathcal{T}, \quad (14)$$

where $f_{ij}^{\text{C}}(t)$ is the computation resource that the j -th UAV can provide to the i -th UE in the t -th time slot.

Note that the time needed for returning the results back to UE from UAV is ignored, similar to [32]. The overall energy consumption of the i -th UE to the j -th UAV in the t -th time slot is given by

$$E_{ij}^{\text{Tr}}(t) = P_i^{\text{Tr}} T_{ij}^{\text{Tr}}(t), \quad t \in \mathcal{T}. \quad (15)$$

If the UE decides to execute the task locally, the power consumption can be evaluated as $k_i (f_{ij}^{\text{L}})^{v_i}(t)$, where $k_i \geq 0$ is the effective switched capacitance, v_i is typically set to 3, and $f_{ij}^{\text{L}}(t)$ is the computation resource that the i -th UE applies to execute the task. The overall time for local execution can be given by

$$T_{ij}^{\text{L}}(t) = \frac{F_i(t)}{f_{ij}^{\text{L}}(t)}. \quad (16)$$

Thus, the total energy consumption for local execution equals

$$E_{ij}^{\text{L}}(t) = k_i (f_{ij}^{\text{L}}(t))^{v_i} T_{ij}^{\text{L}}(t), \quad t \in \mathcal{T}. \quad (17)$$

To sum up, the overall energy consumption for task execution $E_{ij}(t)$ is given by

$$E_{ij}(t) = \begin{cases} E_{ij}^{\text{L}}(t), & \text{local execution} \\ E_{ij}^{\text{Tr}}(t), & \text{offloading} \end{cases} \quad (18)$$

and the time to complete the task $T_{ij}(t)$ is expressed as

$$T_{ij}(t) = \begin{cases} T_{ij}^{\text{L}}(t), & \text{local execution} \\ T_{ij}^{\text{O}}(t), & \text{offloading.} \end{cases} \quad (19)$$

Without loss of generality, we assume that each task has to be completed within the time duration T^{\max} , which is consistent with the maximal flying time in each time slot, given by (7). Then, one has

$$T_{ij}(t) \leq T^{\max}, \forall i \in \mathcal{N}, j \in \mathcal{M}', t \in \mathcal{T}. \quad (20)$$

In each time slot, since the computation resource that each UAV can provide is limited, we have

$$\sum_{i=1}^N a_{ij}(t) f_{ij}^C(t) \leq f_j^{\max}(t), \forall j \in \mathcal{M}, t \in \mathcal{T}, \quad (21)$$

where $f_j^{\max}(t)$ is the maximal computation resource that the j -th UAV can provide in the t -th time slot. Next, we show our proposed problem formulation.

C. Problem Formulation

Denote $\mathbf{U} = \{\theta_j(t), d_j(t), \forall j \in \mathcal{M}, t \in \mathcal{T}\}$, $\mathbf{A} = \{a_{ij}(t), \forall i \in \mathcal{N}, j \in \mathcal{M}', t \in \mathcal{T}\}$, $\mathbf{F} = \{f_{ij}(t), \forall i \in \mathcal{N}, j \in \mathcal{M}', t \in \mathcal{T}\}$. Then, the energy minimization for all UEs is formulated as

$$\mathcal{P}1 : \min_{\mathbf{U}, \mathbf{A}, \mathbf{F}} \sum_{i=1}^N \sum_{j=0}^M \sum_{t=1}^T a_{ij}(t) E_{ij}(t) \quad (22a)$$

subject to:

$$a_{ij}(t) \in \{0, 1\}, \forall i \in \mathcal{N}, j \in \mathcal{M}', t \in \mathcal{T}, \quad (22b)$$

$$\sum_{j=0}^M a_{ij}(t) = 1, \forall i \in \mathcal{N}, t \in \mathcal{T}, \quad (22c)$$

$$0 \leq \theta_j(t) \leq 2\pi, \forall j \in \mathcal{M}, t \in \mathcal{T}, \quad (22d)$$

$$0 \leq d_j(t) \leq d_j^{\max}, \forall j \in \mathcal{M}, t \in \mathcal{T}, \quad (22e)$$

$$\sum_{i=1}^N a_{ij}(t) \leq V_j^{\max}, \forall j \in \mathcal{M}, t \in \mathcal{T}, \quad (22f)$$

$$a_{ij}(t) R_{ij}(t) \leq R_j^{\max}, \forall i \in \mathcal{N}, j \in \mathcal{M}, t \in \mathcal{T}, \quad (22g)$$

$$T_{ij}(t) \leq T^{\max}, \forall i \in \mathcal{N}, j \in \mathcal{M}', t \in \mathcal{T}, \quad (22h)$$

$$\sum_{i=1}^N a_{ij}(t) f_{ij}^C(t) \leq f_j^{\max}(t), \forall j \in \mathcal{M}, t \in \mathcal{T}. \quad (22i)$$

One can see that the above problem $\mathcal{P}1$ is a mixed integer nonlinear programming (MINLP), as it includes both integer variable, \mathbf{A} and continuous variables, \mathbf{F} and \mathbf{U} , which is very difficult

to solve in general. We first propose a convex optimization based algorithm CAT to address it iteratively. Then, we propose a Deep Reinforcement Learning (DRL) based RAT to facilitate fast decision-making, which can be applied in dynamic environment. Note that in practice, if the i -th UE does not generate the tasks in the t -th time slot and then the corresponding $D_i(t)$ and $F_i(t)$ can be set to zero.

IV. PROPOSED CAT ALGORITHM

In this section, a convex optimization based CAT is proposed to solve the above problem $\mathcal{P}1$. We first define a set of new variables to denote the trajectories of UAVs as $\mathbf{G} = \{G_j(t), \forall j \in \mathcal{M}, t \in \mathcal{T}\}$, where the coordinates are $G_j(t) = [X_j(t), Y_j(t)]$, $X_j(t) = X_j(0) + \sum_{l=1}^t d_j(l)\cos\theta_j(l)$ and $Y_j(t) = Y_j(0) + \sum_{l=1}^t d_j(l)\sin\theta_j(l)$. Thus, the optimization problem $\mathcal{P}1$ can be reformulated as

$$\mathcal{P}2 : \min_{\mathbf{G}, \mathbf{A}, \mathbf{F}} \sum_{i=1}^N \sum_{j=0}^M \sum_{t=1}^T a_{ij}(t)E_{ij}(t) \quad (23a)$$

subject to: (22b), (22c), (22f), (22h), (22i),

$$a_{ij}(t)\|G_j(t) - q_i\|^2 \leq (R_j^{\max})^2, \forall i \in \mathcal{N}, j \in \mathcal{M}, t \in \mathcal{T}, \quad (23b)$$

$$\|G_j(t+1) - G_j(t)\|^2 \leq (d_j^{\max})^2, \forall t \in \{1, 2, \dots, T-1\}, \quad (23c)$$

where $q_i = [x_i, y_i]$. In order to solve $\mathcal{P}2$, we divide it into two subproblems and apply the block coordinate descent (BCD) method to address it. To this end, we first optimize the user association \mathbf{A} and resource allocation \mathbf{F} given the UAV trajectory \mathbf{G} . Then, we optimize the UAV trajectory \mathbf{G} given the user association \mathbf{A} and resource allocation \mathbf{F} . We solve the two optimization problems iteratively, until the convergence is achieved.

A. User Association and Resource Allocation

Given the UAV trajectory \mathbf{G} , the subproblem to decide user association \mathbf{A} and resource allocation \mathbf{F} can be formulated as

$$\min_{\mathbf{A}, \mathbf{F}} \sum_{i=1}^N \sum_{j=0}^M \sum_{t=1}^T a_{ij}(t)E_{ij}(t) \quad (24a)$$

subject to: (22b), (22c), (22f), (22h), (22i), (23b).

One can see that (22h) can be written as

$$f_{ij}^C(t) \geq \frac{F_i(t)}{T^{\max} - \frac{D_i(t)}{r_{ij}(t)}}, \quad \forall j \in \mathcal{M}, t \in \mathcal{T}, \quad (25)$$

if the i -th UE chooses to offload the task, and

$$f_{ij}^L(t) \geq \frac{F_i(t)}{T^{\max}}, \quad j = 0, \forall t \in \mathcal{T}. \quad (26)$$

if the i -th UE decides to execute the task locally. It is readily to see that equality holds for both (25) and (26).

Then, (24) can be re-written as

$$\min_{\mathbf{A}, \mathbf{F}} \sum_{i=1}^N \sum_{j=0}^M \sum_{t=1}^T \left(a_{ij}(t) E_{ij}^{\text{Tr}}(t) + (1 - a_{ij}(t)) E_{ij}^L(t) \right) \quad (27a)$$

subject to: (22b), (22c), (22f), (23b),

$$f_{ij}^L(t) = \frac{F_i(t)}{T^{\max}}, \quad j = 0, \forall t \in \mathcal{T}, \quad (27b)$$

$$\sum_{i=1}^N a_{ij}(t) \frac{F_i(t)}{T^{\max} - \frac{D_i(t)}{r_{ij}(t)}} \leq f_j^{\max}(t), \quad \forall j \in \mathcal{M}, t \in \mathcal{T}. \quad (27c)$$

It is readily to find that (27) is a Multiple-Choice Multi-Dimensional 0-1 Knapsack Problem (MMKP), which is NP-hard in general. Fortunately, it can be solved by applying Branch and Bound method via a standard Python package PULP [33].

B. UAV Trajectory Optimization

Given the user association and resource allocation from (27) and removing the constant, $\mathcal{P}2$ can be simplified as

$$\min_{\mathbf{G}} \sum_{i=1}^N \sum_{j=1}^M \sum_{t=1}^T a_{ij}(t) \frac{P_i^{\text{Tr}} D_i(t)}{B \log_2 \left(1 + \frac{\alpha P_i^{\text{Tr}}}{H_j^2 + \|G_j(t) - q_i\|^2} \right)} \quad (28a)$$

subject to: (23b), (23c),

$$\frac{D_i(t)}{B \log_2 \left(1 + \frac{\alpha P_i^{\text{Tr}}}{H_j^2 + \|G_j(t) - q_i\|^2} \right)} + \frac{F_i(t)}{f_{ij}^C(t)} \leq T^{\max}, \quad \forall i \in \mathcal{N}, j \in \mathcal{M}, t \in \mathcal{T}. \quad (28b)$$

It is easy to see that the above optimization problem is non-convex with respect to $G_j(t)$. Next, we introduce a set $\boldsymbol{\eta} = \{\eta_{ij}(t), \forall i \in \mathcal{N}, j \in \mathcal{M}, t \in \mathcal{T}\}$, where $\eta_{ij}(t) = a_{ij}(t) \frac{P_i^{\text{Tr}} D_i(t)}{B \log_2 \left(1 + \frac{\alpha P_i^{\text{Tr}}}{H_j^2 + \|G_j(t) - q_i\|^2} \right)}$, then, problem (28) can be transformed into

$$\min_{\mathbf{G}, \boldsymbol{\eta}} \sum_{i=1}^N \sum_{j=1}^M \sum_{t=1}^T \eta_{ij}(t) \quad (29a)$$

subject to: (23b), (23c),

$$a_{ij}(t) B \log_2 \left(1 + \frac{\alpha P_i^{\text{Tr}}}{H_j^2 + \|G_j(t) - q_i\|^2} \right) \geq \frac{P_i^{\text{Tr}} D_i(t)}{\eta_{ij}(t)}, \forall i \in \mathcal{N}, j \in \mathcal{M}, t \in \mathcal{T} \quad (29b)$$

$$B \log_2 \left(1 + \frac{\alpha P_i^{\text{Tr}}}{H_j^2 + \|G_j(t) - q_i\|^2} \right) \geq \frac{D_i(t)}{T^{\max} - \frac{F_i(t)}{f_{ij}^c(t)}}, \forall i \in \mathcal{N}, j \in \mathcal{M}, t \in \mathcal{T}. \quad (29c)$$

One observes that (29b) and (29c) are convex with respect to $\|G_j(t) - q_i\|$, respectively. Thus, (29b) and (29c) are non-convex constraints. Then, similar to [4], [5], we apply the successive convex approximation (SCA) to solve this problem. Specifically, for any given local point $G_j^r(t)$ in $\mathbf{G}^r = \{G_j^r(t), \forall j \in \mathcal{M}, t \in \mathcal{T}\}$, one can have the following inequality as

$$\begin{aligned} w_{ij}(t) &= B \log_2 \left(1 + \frac{\alpha P_i^{\text{Tr}}}{H_j^2 + \|G_j(t) - q_i\|^2} \right) \\ &\geq K_{ij}^r(t) (\|G_j(t) - q_i\|^2 - \|G_j^r(t) - q_i\|^2) + B_{ij}^r(t) \triangleq w_{ij}^{lb,r}(t), \end{aligned} \quad (30)$$

where

$$K_{ij}^r(t) = -\frac{B \alpha P_i^{\text{Tr}} \log_2(e)}{(H_j^2 + \|G_j^r(t) - q_i\|^2)(H_j^2 + \|G_j^r(t) - q_i\|^2 + \alpha P_i^{\text{Tr}})}, \quad (31)$$

and

$$B_{ij}^r(t) = \log_2 \left(1 + \frac{\alpha P_i^{\text{Tr}}}{H_j^2 + \|G_j^r(t) - q_i\|^2} \right), \forall j \in \mathcal{M}, t \in \mathcal{T}. \quad (32)$$

Then, problem (29) can be written as

$$\min_{\mathbf{G}, \boldsymbol{\eta}} \sum_{i=1}^N \sum_{j=1}^M \sum_{t=1}^T \eta_{ij}(t) \quad (33a)$$

subject to: (23b), (23c),

$$a_{ij}(t) w_{ij}^{lb,r}(t) \geq \frac{P_i^{\text{Tr}} D_i(t)}{\eta_{ij}(t)}, \forall i \in \mathcal{N}, j \in \mathcal{M}, t \in \mathcal{T}, \quad (33b)$$

$$w_{ij}^{lb,r}(t) \geq \frac{D_i(t)}{T^{\max} - \frac{F_i(t)}{f_{ij}^c(t)}}, \forall i \in \mathcal{N}, j \in \mathcal{M}, t \in \mathcal{T}. \quad (33c)$$

The above problem is a convex quadratically constrained quadratic program (QCQP) and it can be solved by a standard Python package CVXPY [34].

C. Overall Algorithm Design

In this section, a convex optimization algorithm based CAT is proposed to solve Problem $\mathcal{P}2$, where we optimize user association and resource allocation subproblem iteratively with the UAV trajectory subproblem until the convergence is achieved. We describe the pseudo code of proposed CAT in Algorithm 1.

Algorithm 1 CAT Algorithm

- 1: Set $r = 0$, and initialize \mathbf{G}^r ;
 - 2: **repeat**
 - 3: Solve Problem (27) by Branch and Bound method for given \mathbf{G}^r , and denote the optimal solution as \mathbf{A}^{r+1} and \mathbf{F}^{r+1} ;
 - 4: Solve Problem (33) for given \mathbf{A}^{r+1} and \mathbf{F}^{r+1} , and denote the solution as \mathbf{G}^{r+1} ;
 - 5: $r = r + 1$;
 - 6: **until** the convergence is achieved.
-

Discussions: Algorithm 1 needs to run once the initial taking-off locations of the UAVs change. However, the complexity of Algorithm 1 is high as the solutions are iteratively obtained and each subproblem involves a huge number of optimization variables especially when the total number of time slots is high. Hence, Algorithm 1 is not suitable for some emergence scenarios (e.g., battlefields, earthquake, large fires), where fast decision making is highly demanded. This motivates the algorithm developed based on DRL in the following section.

V. PROPOSED RAT ALGORITHM

To facilitate the fast decision making, the DRL-based RAT algorithm is proposed in this section. We first give some preliminaries as follows.

A. Preliminaries

1) *DQN*: In a standard reinforcement learning, an agent is assumed to interact with the environment and select the optimal action that can maximize the accumulated reward. In [28], a Deep Q Network (DQN) structure developed by Google Deepmind, integrates the deep neural networks with traditional reinforcement learning. The DQN is used to estimate the well-known Q-value defined as

$$Q(s(t), c(t)) = \mathbb{E}[Z(t)|s(t), c(t)], \quad (34)$$

where $s(t)$ and $c(t)$ denote the state and action respectively, $\mathbb{E}[\cdot]$ denotes the expectation, whereas $Z(t) = \sum_{t'=t}^T \gamma z(t')$ is a reward and $\gamma \in [0, 1]$ is the discount factor and $z(t')$ is a reward function in the t' -th time step (or time slot). As the objective is to maximize the reward, a widely used policy is $\pi(s(t)|\phi^Q) = \operatorname{argmax}_{c(t)} Q(s(t), c(t)|\phi^Q)$, where ϕ^Q is the parameter of the deep neural network. Then, the DQN can be trained by minimizing the loss function [28]. Also, since the deep networks are known to be unstable and very difficult to converge, two effective approaches, i.e., target network and experience replay, have been introduced in [28]. The target network has the same structure as the original DQN but the parameters are updated more slowly. The experience replay stores the state transition samples which can help the DQN converge. However, the DQN was originally designed to solve the problem with discrete variables. Although we can adapt the DQN to continuous problems by discretizing the action space, it may unfortunately result in a huge searching space and therefore intractable to deal with.

2) *DDPG*: To deal with the problem with continuous variables, e.g., the trajectory control of UAV, one may apply the actor-critic approach, which was developed in [35]. DeepMind has proposed a deep deterministic policy gradient (DDPG) approach [30] by integrating the actor-critic approach into DRL. DDPG includes two DQNs, one of the DQNs, named actor network with function $\pi(s(t)|\phi^\pi)$ is applied to generate action $c(t)$ for a given state $s(t)$. The other DQN named critic network with function $Q(s(t), c(t)|\phi^Q)$, is used to generate the Q-value, which evaluates the action produced by the actor network. In order to improve the learning stability, two adjacent target networks corresponding to the actor and critic networks, $\pi'(\cdot)$, $Q'(\cdot)$ with respective parameters $\phi^{\pi'}$, $\phi^{Q'}$, are also applied.

Then, the critic network can be updated with the loss function, $L(\phi^Q)$, as

$$L(\phi^Q) = \frac{1}{K} \sum_{k=1}^K \delta_k^2, \quad (35)$$

where in each time step we obtain K samples constituting mini-batch from the experience replay buffer, and δ_k is the temporal difference (TD)-error [36] which is given by

$$\delta_k = z(k) + \gamma Q'(s(k+1), \pi'(s(k+1)|\phi^{\pi'})|\phi^{Q'}) - Q(s(k), \pi(s(k)|\phi^\pi)|\phi^Q). \quad (36)$$

On the other hand, the actor network can be updated by applying the policy gradient, which

is described as [30].

$$\begin{aligned}\nabla_{\phi^\pi} J &\approx \frac{1}{K} \sum_{k=1}^K \nabla_c Q(s, c | \phi^Q)|_{s=s(k), c=\pi(s(k)|\phi^\pi)} \\ &= \frac{1}{K} \sum_{k=1}^K \left[\nabla_c Q(s, c | \phi^Q)|_{s=s(k), c=\pi(s(k))} \cdot \nabla_{\phi^\pi} \pi(s | \phi^\pi)|_{s=s(k)} \right].\end{aligned}\quad (37)$$

B. The RAT Algorithm

In this section, we introduce the DRL based RAT algorithm, which includes deep neural networks (i.e., actor and critic networks) and the matching algorithms. In order to apply the DRL, we first define the state, action and reward as follows:

- 1) **State** $s(t)$: $s(t) = \{[X_1(t), Y_1(t), H_1], [X_2(t), Y_2(t), H_2], \dots, [X_M(t), Y_M(t), H_M]\}$, $s(t)$ is the set of the coordinates of all UAVs.
- 2) **Action** $c(t)$: $c(t)$ is the set of the actions of all UAVs, including the flying direction $\theta_j(t)$ and distance $d_j(t)$. Since the absolute operation of $\tanh(\cdot)$ is used as the activation function, it means the output value of the DQN is within the interval $[0, 1]$. Thus, the flying direction and distance are reformulated as $\theta_j(t) = 2\pi\lambda_j(t)$ and $d_j(t) = \alpha_j(t)d_j^{\max}$, where

$$0 \leq \lambda_j(t) \leq 1, \forall j \in \mathcal{M}, t \in \mathcal{T}, \quad (38)$$

and

$$0 \leq \alpha_j(t) \leq 1, \forall j \in \mathcal{M}, t \in \mathcal{T}. \quad (39)$$

Then, the action set can be defined as $c(t) = \{[\lambda_1(t), \alpha_1(t)], [\lambda_2(t), \alpha_2(t)], \dots, [\lambda_M(t), \alpha_M(t)]\}$.

- 3) **Reward** $z(t)$: $z(t)$ is defined as the minus of the overall energy consumption of all the UEs in each time slot as

$$z(t) = - \sum_{i=1}^N \sum_{j=0}^M a_{ij}(t) E_{ij}(t). \quad (40)$$

The algorithm framework used in this paper is depicted in Fig. 2, where an agent, which could be deployed in the central control center in the base station, is assumed to interact with the environment. An actor network $\pi(s(t)|\phi^\pi)$ is applied to generate the action, which includes the flying direction and distance for each UAV. The critic network $Q(s(t), c(t)|\phi^Q)$ is used to obtain the Q value of the action (i.e., to evaluate the actions generated by actor networks). In each time slot, the agent generates the actions for all the UAVs (including moving direction and distance). Then, each UE tries to associate with one UAV in its coverage, i.e., (10) by using a

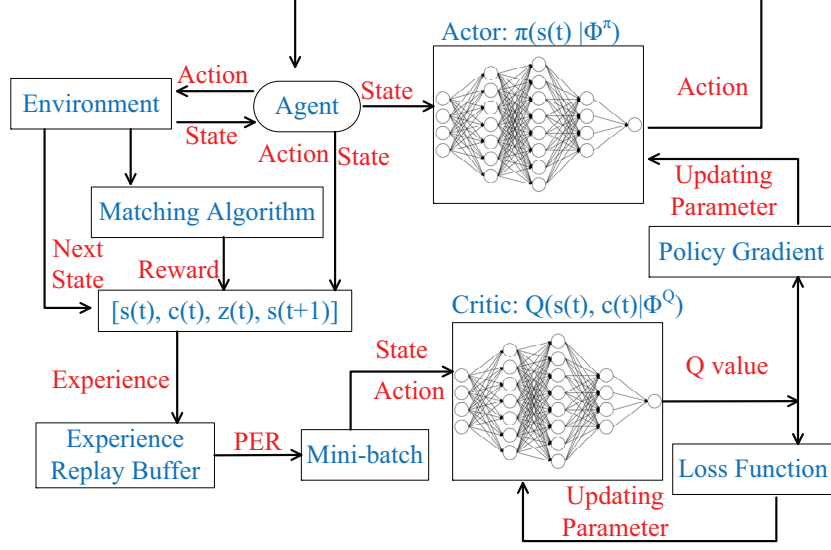


Fig. 2: The networks applied in this paper.

matching algorithm in Algorithm 3. More specifically, each UE tries to connect the UAV which has the least offloading energy. If the minimum offloading energy is larger than the energy of local execution, the UE will decide to conduct the task locally. Note that RAT has the same optimization strategy for resource allocation as CAT.

Also, each UAV selects the UEs based on the following criteria: 1) UE should be in its coverage area; 2) UE with the smaller resource requirement, i.e., $f_{ij}^C(t)$ will be given higher priority in offloading to this UAV. We will introduce the details of the proposed matching algorithm in Algorithm 2. After the matching algorithm, the reward in (40) can be obtained.

We assume that there is an experience replay buffer \mathcal{X} for the agent to store the experience $[s(t), c(t), z(t), s(t+1)]$. Once the experience replay buffer is full, the learning procedure starts. A mini-batch \mathcal{K} with size K can be obtained from the experience replay buffer to train the networks.

In the classical DRL algorithms, such as Q-learning [37], SARSA [38] and DDPG [30], the mini-batch uniformly samples experiences from the experience replay buffer. However, since TD-error in (36) is used to update the Q value network, experience with high TD-error often indicates the successful attempts. Therefore, a better way to select the experience is to assign different weights to samples. Schaul *et al.* [31] developed a prioritized experience replay scheme, in which

the absolute TD-error $|\delta_k|$ is used to evaluate the probability of the sampled k -th experience from the mini-batch. Then, the probability of sampling the k -th experience can be given by

$$P(k) = \frac{(p_k)^\beta}{\sum_{m \in K} p_m^\beta} \quad (41)$$

where $p_k = |\delta_k| + \epsilon$, $\epsilon = 0.001$ is a positive constant to avoid the edge-case of transitions not being revisited if $|\delta_k|$ is 0, $\beta = 0.6$ is denoted as a factor to determine the prioritization [31].

However, frequently sampling experiences with high $|\delta_k|$ can cause divergence and oscillation. To tackle this issue, the importance-sampling weight [39] is introduced to represent the importance of sampled experience, which can be given by

$$\omega_k = \frac{1}{(x \cdot P(k))^\mu} \quad (42)$$

where x is the size of experience replay buffer \mathcal{X} , μ is given as 0.4 [31]. Thus, the loss function $L(\phi^Q)$ in (35) can be updated as

$$L(\phi^Q) = \frac{1}{K} \sum_{k=1}^K \omega_k (\delta_k)^2 \quad (43)$$

which is used in our proposed RAT to train the networks. Next, we describe the pseudo code of the overall RAT framework in Algorithm 2.

We first initialize the actor, critic, two target networks, and experience replay buffer in Line 1 - 3. At each epoch, the taking off points of all UAVs are randomly generated in the square area of UEs. We add a random noise N' to the action, where N' follows a normal distribution with 0 mean and variance 1, ρ is set to 3 and decays with a rate of 0.9995 in each time step. From Line 8-11, each UAV flies according to the generated action $c(t)$ and enters the next state $s(t+1)$. Then, we obtain the user association by using Algorithm 3. Next, the reward $z(t)$ is obtained according to (40) (i.e., Line 13). The experience is also stored in the replay buffer \mathcal{X} . When \mathcal{X} is full, the mini-batch samples K experiences by applying the prioritized experience replay (i.e., Line 16-19). Then, we update the actor and critic networks by using loss function in (43) and policy gradient in (37) respectively. Finally, we update the target networks by using the following equations as (i.e., Line 22)

$$\phi^{Q'} \leftarrow \tau \phi^Q + (1 - \tau) \phi^{Q'} \quad (44)$$

and

$$\phi^{\pi'} \leftarrow \tau \phi^\pi + (1 - \tau) \phi^{\pi'} \quad (45)$$

Algorithm 2 RAT Algorithm

- 1: Initialize actor network $\pi(s(t)|\phi^\pi)$ with parameters ϕ^π and critic network $Q(s(t), s(t)|\phi^Q)$ with parameters ϕ^Q ;
 - 2: Initialize target networks $Q'(\cdot)$ with parameters $\phi^{Q'} = \phi^Q$ and $\pi'(\cdot)$ with parameters $\phi^{\pi'} = \phi^\pi$;
 - 3: Initialize experience replay buffer \mathcal{X} ;
 - 4: **for** epoch = 1, ..., e^{max} **do**
 - 5: Initialize $s(t)$;
 - 6: **for** time step $t = 1, \dots, T$ **do**
 - 7: $\pi(s(t)|\phi^\pi) + \rho N'$ where N' is the random noise and ρ decays with t ;
 - 8: **for** UAV $j = 1, \dots, M$ **do**
 - 9: Execute $c(t)$;
 - 10: Obtain $s(t + 1)$;
 - 11: **end for**
 - 12: Obtain the user association with UAVs using matching algorithm proposed in Algorithm 3;
 - 13: Obtain the reward $z(t)$ from (40);
 - 14: Store experience $[s(t), c(t), z(t), s(t + 1)]$ into \mathcal{X} ;
 - 15: **if** \mathcal{X} is full **then**
 - 16: **for** $k = 1, \dots, K$ **do**
 - 17: Sample k -th experience with probability $P(k)$ from (41);
 - 18: Calculate $|\delta_k|$ and ω_k from (36) and (42) respectively;
 - 19: **end for**
 - 20: Update parameters of the critic network ϕ^Q by minimizing its loss function according to (43);
 - 21: Update parameters of the actor network ϕ^π by using policy gradient approach according to (37);
 - 22: Update two target networks with the updating rate τ ;
 - 23: **end if**
 - 24: **end for**
 - 25: **end for**
-

where τ is the updating rate.

Algorithm 3 Matching Algorithm

```

1: Initialize  $\mathbf{A}$  and  $\mathbf{F}_j, \forall j \in \mathcal{M}, \forall i \in \mathcal{N}$ ;
2: for UAV  $j = 1, \dots, M$  do
3:   for UE  $i = 1, \dots, N$  do
4:     if (10) is met then
5:       Calculate  $E_{ij}^L(t), E_{ij}^{\text{Tr}}(t)$  and  $f_{ij}^C(t)$ ;
6:       if  $E_{ij}^L(t) > E_{ij}^{\text{Tr}}(t)$  then
7:         Store  $i$  into  $\mathbf{F}_j$ ;
8:       end if
9:     end if
10:  end for
11:  Sort the element in  $\mathbf{F}_j$  in ascending order with respect to  $f_{ij}^C(t)$ ;
12: end for
13: repeat
14: for UAV  $j = 1, \dots, M$  do
15:    $i = \text{GetTopItem}(\mathbf{F}_j)$ ;
16:   if (8), (21) are met then
17:     if  $E_{ij}^{\text{Tr}}(t) < E_{iA(i)}^{\text{Tr}}(t)$  or  $\mathbf{A}(i) = 0$  then
18:        $\mathbf{A}(i) = j$ ;
19:     end if
20:      $\text{RemoveTopItem}(\mathbf{F}_j)$ ;
21:   end if
22: end for
23: until Each UE in  $\mathbf{F}_j$  is checked.
24: Return  $\mathbf{A}$ 

```

Next, we introduce the low-complexity matching algorithm which can decide the user association and resource allocation given UAVs' trajectory, as shown in Algorithm 3. First, we denote \mathbf{A} with size N to record the user association between UEs and UAVs. If $\mathbf{A}(i) = j$, it means the i -th UE matches with the j -th UAV, and if $\mathbf{A}(i) = 0$, it denotes that the i -th UE is not matched yet and has to execute its task locally. In addition, we denote a preference list \mathbf{F}_j

for the j -th UAV to record UEs that can benefit from offloading. Then, from Line 2 to 10, we generate the preference list F_j for the j -th UAV. Precisely, if constraint (10) is met, we obtain $E_{ij}^L(t)$, $E_{ij}^{\text{Tr}}(t)$ and $f_{ij}^C(t)$ according to (17), (15), and (25), respectively. UEs that benefit from offloading will be stored in F_j . Since UAVs wish to accept as many UEs as possible, we sort the preference list F_j with ascending order with respect to $f_{ij}^C(t)$, as shown in Line 11. The UE that consumes less $f_{ij}^C(t)$ will be matched with a higher priority. Next, from Line 13 to 23, we conduct the matching process. Each UAV keeps selecting UEs according to its preference list, and constantly checking the constraints (8) and (21) based on \mathbf{A} . In the meantime, the selected UE will determine whether to match with the UAV or not. Precisely, from Line 17 to 19, if the selected UE is not matched before, or matching with the j -th UAV could save more energy than previous match, the corresponding $A(i)$ will be updated. We do this process until all the UEs in each preference list are checked. Then, the final user association can be obtained from \mathbf{A} .

Once the whole networks are converged, the solutions can be generated very fast with only some simple algebraic calculations instead of solving the original MINLP. This is due to the fact that during the training stages, random taking off points of all the UAVs are generated and the networks are trained to converge.

VI. SIMULATION RESULTS

In this section, both convex optimization based CAT and DRL based RAT are evaluated with simulations. CAT algorithm is executed by using Python 3.6, PULP 1.6.10, and CVXPY 1.0.24, while RAT are examined by using Tensorflow 1.12.0 with 4 NVIDIA GTX 1070 Ti. We deploy three fully-connected hidden layers with 1024, 800 and 600 neurons in both actor and critic networks in RAT. The actor network is trained by applying RMSPropOptimizer with the learning rate 0.001, whereas the critic network is trained by using AdamOptimizer with the learning rate 0.001. We assume there are 100 time slots in each run and in each time slot, UE generates a task with communication requirement $D_i(t) \in [100, 1000]$ KB and computation requirement $F_i(t) \in [10^8, 10^9]$ cycles. Other parameters are summarized in Table II. We assume in each time slot, UAVs will send a signal to activate the corresponding UEs, which will either offload the task or execute locally, within the delay requirement.

In order to evaluate the performance of the proposed CAT and RAT, we present the following three algorithms for comparison purpose.

- **Local Execution (LE):** All tasks are executed locally without offloading.

TABLE II: Simulation Parameters

Parameters	Settings	Parameters	Settings
\mathcal{T}	100	g_0	1.42×10^{-4}
d_j^{\max}	30 m	V_j^{\max}	40
v_j	30 m/s	T^{\max}	1 s
R_j^{\max}	100 m	f_j^{\max}	50 GHz
H_j	100 m	k_i for all UEs	10^{-27}
B	1 MHz	Size of experience replayer buffer \mathcal{X}	10^5
$P_{ij}^{\text{Tr}}(t)$	0.1 W	Discount factor γ	0.999
σ^2	-90 dbm/Hz	Iteration number r	10

- **Circle flying (CC):** We group all the UEs into clusters based on the UEs' positions (i.e., two clusters for two UAVs in Fig. 8 and four clusters for four UAVs in Fig. 9). Then, each UAV flies in a circle around each cluster center respectively with radius of R_j^{\max} .
- **Cluster moving (CM):** We group all the UEs into ten clusters and each UAV flies in the trajectory connecting all the cluster center one by one.
- **Deep Deterministic Policy Gradient (DDPG) [30]:** We set the parameter of DDPG the same as actor and critic networks of RAT, but do not apply the prioritized experience replay. In other words, DDPG uniformly samples the experiences from the experience replay buffer in the training procedure.

Note that all the above compared algorithms apply the matching algorithm proposed in Algorithm 3 to decide the user association and resource allocation.

A. Convergence Evaluation of CAT and RAT

In this subsection, we show the convergence of proposed CAT and RAT, where we assume there are 100 UEs randomly distributed in a square area with four coordinates $[0, 0]$, $[0, 200]$, $[200, 0]$ and $[200, 200]$ m. In Fig. 3, we show the convergence performance of CAT, where the initial trajectories are set as follows: All the UEs are divided into two clusters according to their positions and two UAVs respectively fly in a circle around the cluster centers with radius R_j^{\max} . One can see from Fig. 3 that the proposed CAT algorithm converges in around 11 iterations.

Then, we show the convergence performance of training process in RAT. The initial coordinates of UAVs are randomly chosen in the square area to train the network to converge. From Fig. 4 to Fig. 5, we compare the influence of hyperparameters to both DDPG and RAT. Prioritized

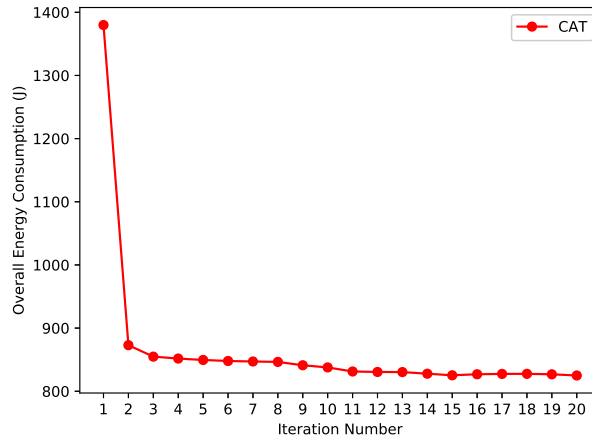
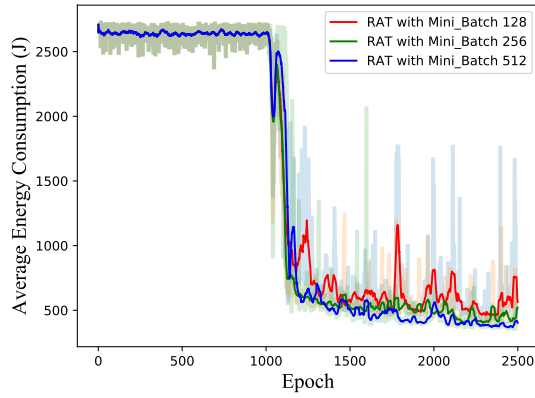


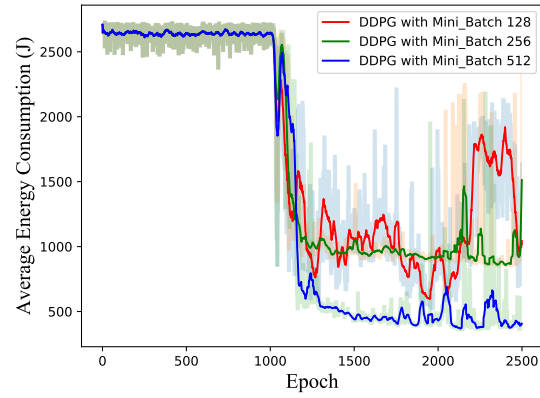
Fig. 3: The convergence performance of proposed CAT.

experience replay is applied in RAT. Both RAT and DDPG start the learning procedure once the experience replay buffer is full. In Fig. 4, we depict the average energy consumption of RAT and DDPG for different size of mini-batches. To be more specific, from Fig. 4a, we can see that RAT has the similar convergence performance for different size of mini-batches and it becomes more stable during the learning procedure. In Fig. 4b, when mini-batch is 128, DDPG has an obvious fluctuation during the learning procedure and it gets worse after the 2000-th epoch. When mini-batch is 256, the convergence performance of DDPG is stable but the average energy consumption that it reaches is not optimal. When mini-batch is 512, DDPG has a promising convergence performance, but it starts to fluctuate after the 1700-th epoch. Overall, from Fig. 4, it is clear to see that the RAT is less sensitive to the change of mini-batch than DDPG.

In Fig. 5, we depict the average energy consumption of RAT and DDPG for different sizes of experience replay buffer, where the mini-batch is set as 128. From Fig. 5a and 5b, when experience replay buffer is 50000, although RAT has a fluctuation after the 1000-th epoch, DDPG has no convergence tendency during the entire learning procedure. When experience replay buffer is 70000, the average energy consumption that DDPG can reach is about 1800 J, and DDPG has fluctuations both after the 1500-th epoch and the 2000-th epoch. When experience replay buffer is 100000, it seems that DDPG can reach the good average energy consumption but it does not perform as stable as RAT. To conclude, it is obvious to see that RAT is less

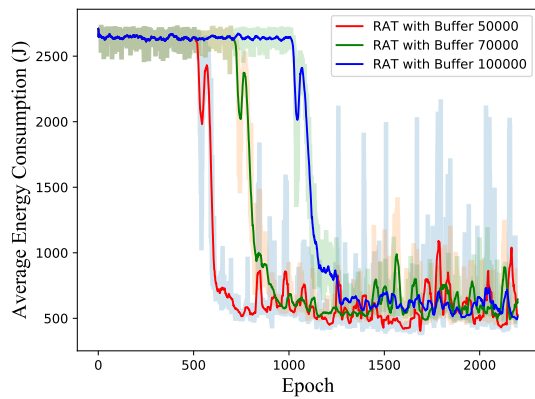


(a) The average energy consumption of RAT with different batch size.

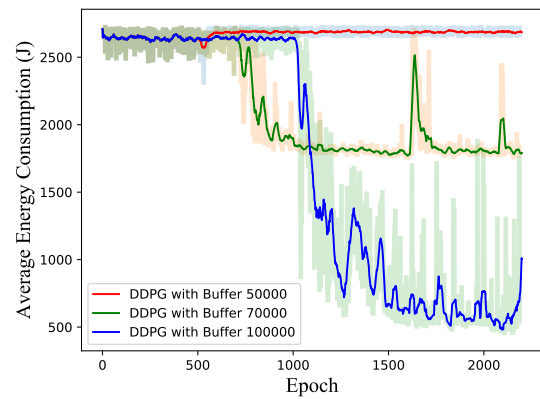


(b) The average energy consumption of DDPG with different batch size.

Fig. 4: The convergence performance of RAT and DDPG in different size of mini-batch.



(a) The average energy consumption of RAT with different buffer size.



(b) The average energy consumption of DDPG with different buffer size.

Fig. 5: The convergence performance of RAT and DDPG in different experience replay buffer.

sensitive to the size of experience replay buffer than DDPG.

B. Trajectory Evaluation of CAT and RAT

In Fig. 6 and Fig. 7, we show the trajectories obtained by RAT and CAT, respectively, where we assume there are 100 UEs randomly distributed in a square area with four coordinates $[100, 100]$, $[100, 300]$, $[300, 300]$ and $[300, 100]$ m. Ten initial taking off points of two UAVs are randomly set in the square area with four coordinates $[0, 0]$, $[0, 400]$, $[400, 400]$ and $[400, 0]$ m. For CAT, its initial trajectories are given by RAT. One can see from Fig. 6 and Fig. 7 that no matter where the taking off points of the UAVs are, the proposed RAT and CAT can guide the UAVs to serve the users in the similar trajectory. Note that RAT can obtain the trajectories very fast. This is due to the fact that we train the RAT to converge during the training stage by randomly generating many taking off points of the UAVs. Then, during the testing stages, RAT can intermediately output the best solutions once taking off points are input. Also, note that unlike CAT which may fall into the local optimum, the proposed RAT has the global search ability due to the application of reinforcement learning techniques.

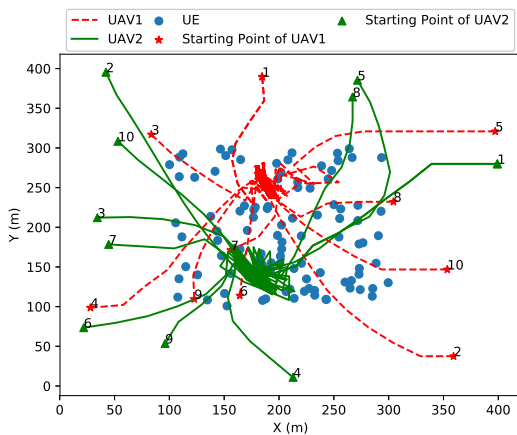


Fig. 6: Multi-UAV enabled F-MEC architecture controlled by RAT.

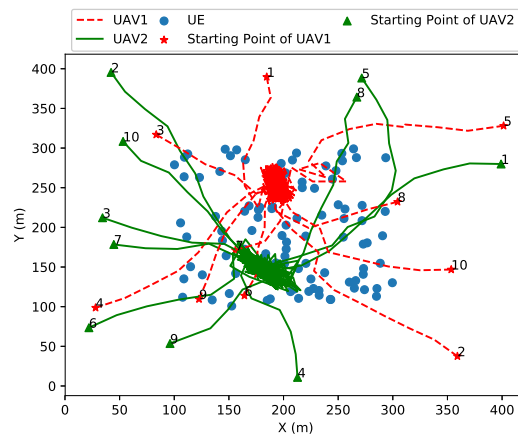


Fig. 7: Multi-UAV enabled F-MEC architecture controlled by CAT.

C. Energy Consumption Evaluation of CAT and RAT

In Fig. 8, we check the performance of LE, CC, CM, CAT, and RAT, where the mini-batch of RAT is set to 128, the learning rate of actor and critic networks of RAT is set to 0.001. Both

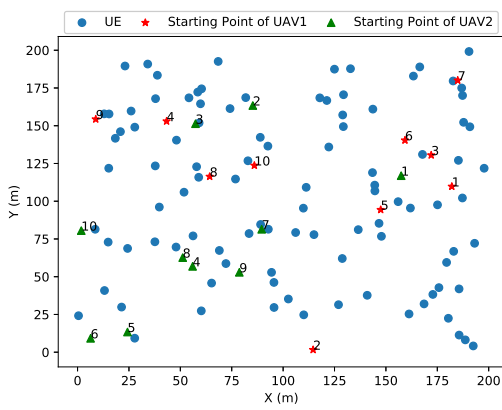
actor and critic networks in RAT are trained for 2500 epochs. All UEs are randomly distributed in the square area with four coordinates $[0, 0]$, $[0, 200]$, $[200, 200]$, and $[200, 0]$ m. The initial trajectories of CAT are given by RAT. We randomly select ten starting points of two UAVs, as shown in Fig. 8a. In Fig. 8b, we depicts the average energy consumption of LE, CM, CC, CAT, and RAT in each time step. One can see that the overall energy consumption varies for all the algorithms in each time slot. This is because we randomly generate the tasks every step. CAT and RAT perform much better when compared with LE, CM, and CC, as expected. Also, one can see that the energy consumption of CC fluctuates in each time step and CM has the fluctuation but it performs better than CC. This is due to the reason that CM benefits from the clustering algorithm and flying between cluster centers could potentially serve more UEs.

In Fig. 8c, we show the energy consumption of LE, CC, CM, CAT, and RAT versus different starting points. One can see that both CAT and RAT perform much better than other compared algorithms, while LE has the worst performance as it instructs all the UEs to execute the tasks locally. CM and CC perform better than LE but their energy consumption vary with the UAVs' starting off coordinates. Moreover, the energy consumption of CAT and RAT are more stable than CC and CM, even if the starting points of UAVs keep changing.

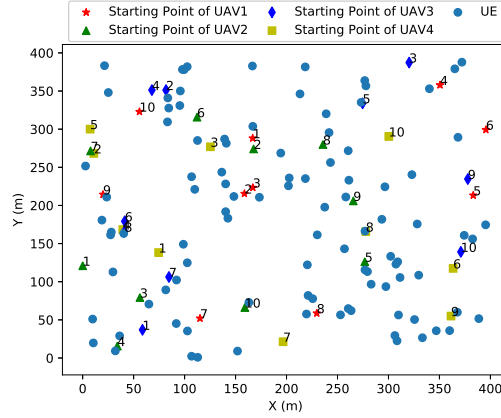
Then, we increase the number of UAVs to four and randomly select ten starting points for each UAV, respectively, as shown in Fig. 9a. The UEs are assumed to randomly distribute in a larger square area with four coordinates $[0, 0]$, $[400, 0]$, $[400, 400]$, and $[0, 400]$ m.

In Fig. 9b, we depict the average energy consumption of LE, CC, CM, CAT, and RAT in each time step. One can see that our proposed CAT and RAT still outperform other compared algorithms, although the energy consumption of CAT and RAT are slightly higher in the first 10 time steps. The performance of CM and CC are better than LE, as expected. Then, we show the energy computation versus different starting points in Fig. 9c. Similar with before, one can see that CAT and RAT significantly reduce the energy consumption for all the UEs. One may notice that compared to two UAVs' scenario before, four UAVs' case costs more energy. This is because four UAVs' scenario are conducted in a larger area.

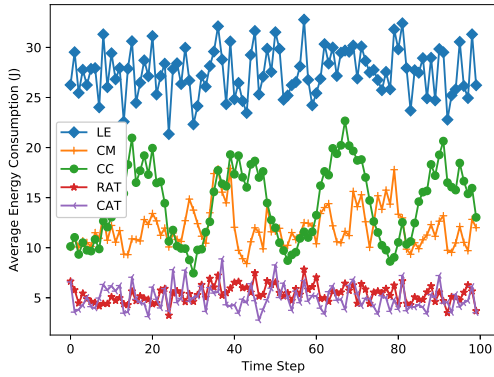
In Table III, we show time consumption consumed by CAR and RAT for each starting point in Fig. 8 and Fig. 9 in our setup. One can see that when the number of UAVs is 2, CAT needs at least 1100 seconds to find a solution, while RAT only needs 1.1 seconds. Also, when the number of UAVs is 4, CAT takes nearly 1200 seconds to obtain a solution while RAT only needs 3.2 seconds in average. This is because for CAT, CVXPY is called in each iteration in



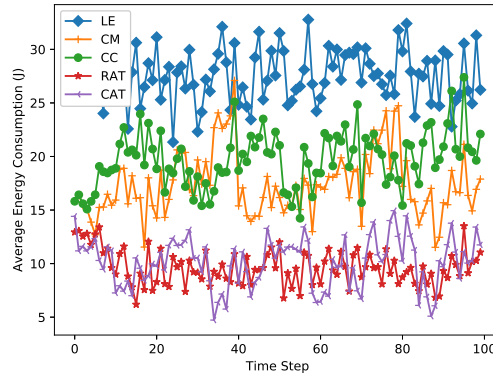
(a) The locations of UEs and the starting off points of two UAVs.



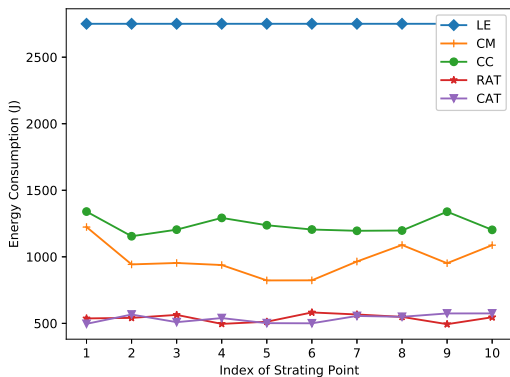
(a) The locations of UEs and the starting off points of four UAVs.



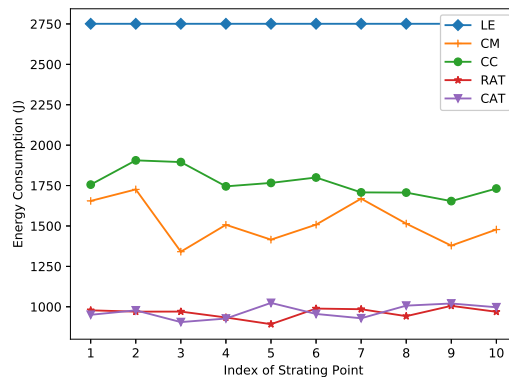
(b) The average energy consumption of LE, CM, CC, CAT, and RAT in different time step.



(b) The average energy consumption of LE, CM, CC, CAT, and RAT in different time step.



(c) The average energy consumption of LE, CM, CC, CAT, and RAT versus different starting off points of two UAVs



(c) The average energy consumption of LE, CM, CC, CAT, and RAT versus different starting off points of four UAVs

Fig. 8: The performance comparison of LE, CM, CC, CAT, and RAT with 2 UAVs.

Fig. 9: The performance comparison of LE, CM, CC, CAT, and RAT with 4 UAVs.

TABLE III: Executed Time of CAT and RAT

Starting Point	UAV = 2		UAV = 4	
	CAT(s)	RAT(s)	CAT(s)	RAT(s)
1	1157.161	1.510	1214.436	3.484
2	1170.661	1.189	1178.298	3.407
3	1148.202	1.185	1202.849	3.239
4	1143.057	1.169	1196.224	3.406
5	1105.217	1.184	1235.483	3.268
6	1039.871	1.179	1335.862	3.301
7	1120.834	1.222	1375.865	3.282
8	1134.115	1.164	1283.899	3.285
9	1120.252	1.166	1332.203	3.262
10	1137.467	1.201	1332.687	3.285

Python. However, the DRL based RAT only needs a few number of algebra calculations once the training is completed offline.

VII. CONCLUSION

In this paper, we consider the flying mobile edge computing architecture, by taking advantage of the UAVs to serve as the moving platform. We aim to minimize the energy consumption of all the UEs by optimizing the UAVs' trajectories, user associations and resource allocation. To tackle the multi-UAVs' trajectories control problem, a convex optimization-based CAT was first proposed. Then, in order to conduct fast decision, a DRL-based RAT including a matching algorithm was also proposed. Simulation results shows that CAT can reach the similar performance as RAT, which confirms the effectiveness of learning based algorithm RAT.

REFERENCES

- [1] Y. C. Hu, M. Patel, D. Sabella, N. Sprecher, and V. Young, "Mobile edge computing—A key technology towards 5G," *ETSI white paper*, vol. 11, no. 11, pp. 1–16, 2015.
- [2] Y. Du, K. Wang, K. Yang, and G. Zhang, "Energy-efficient resource allocation in UAV based MEC system for IoT devices," in *IEEE Global Communications Conference*, 2018, pp. 1–6.
- [3] X. Lyu, H. Tian, W. Ni, Y. Zhang, P. Zhang, and R. P. Liu, "Energy-efficient admission of delay-sensitive tasks for mobile edge computing," *IEEE Trans. Commun.*, vol. 66, no. 6, pp. 2603–2616, June. 2018.
- [4] Q. Wu and R. Zhang, "Common throughput maximization in UAV-enabled ofdma systems with delay consideration," *IEEE Trans. Commun.*, vol. 66, no. 12, pp. 6614–6627, Dec. 2018.

- [5] Z. Li, M. Chen, C. Pan, N. Huang, Z. Yang, and A. Nallanathan, "Joint trajectory and communication design for secure UAV networks," *IEEE Commun. Lett.*, pp. 1–4, Feb. 2019.
- [6] C. H. Liu, Z. Chen, J. Tang, J. Xu, and C. Piao, "Energy-efficient UAV control for effective and fair communication coverage: A deep reinforcement learning approach," *IEEE J. Select. Areas Commun.*, vol. 36, no. 9, pp. 2059–2070, Sep. 2018.
- [7] L. Kong, L. Ye, F. Wu, M. Tao, G. Chen, and A. V. Vasilakos, "Autonomous relay for millimeter-wave wireless communications," *IEEE J. Select. Areas Commun.*, vol. 35, no. 9, pp. 2127–2136, 2017.
- [8] P. Zhan, K. Yu, and A. L. Swindlehurst, "Wireless relay communications with unmanned aerial vehicles: Performance and optimization," *IEEE Transactions on Aerospace and Electronic Systems*, vol. 47, no. 3, pp. 2068–2085, July 2011.
- [9] R. Fan, J. Cui, S. Jin, K. Yang, and J. An, "Optimal node placement and resource allocation for UAV relaying network," *IEEE Communications Letters*, vol. 22, no. 4, pp. 808–811, 2018.
- [10] U. Challita, A. Ferdowsi, M. Chen, and W. Saad, "Machine learning for wireless connectivity and security of cellular-connected UAVs," *IEEE Wireless Communications*, vol. 26, no. 1, pp. 28–35, 2019.
- [11] C. Zhan, Y. Zeng, and R. Zhang, "Energy-efficient data collection in UAV enabled wireless sensor network," *IEEE Wireless Communications Letters*, vol. 7, no. 3, pp. 328–331, June 2018.
- [12] J. Gong, T.-H. Chang, C. Shen, and X. Chen, "Aviation time minimization of UAV for data collection from energy constrained sensor networks," in *2018 IEEE Wireless Communications and Networking Conference (WCNC)*. IEEE, 2018, pp. 1–6.
- [13] J. Lyu, Y. Zeng, and R. Zhang, "UAV-aided offloading for cellular hotspot," *IEEE Transactions on Wireless Communications*, vol. 17, no. 6, pp. 3988–4001, 2018.
- [14] J. Gu, T. Su, Q. Wang, X. Du, and M. Guizani, "Multiple moving targets surveillance based on a cooperative network for multi-UAV," *IEEE Communications Magazine*, vol. 56, no. 4, pp. 82–89, 2018.
- [15] J. Xu, Y. Zeng, and R. Zhang, "UAV-enabled wireless power transfer: Trajectory design and energy optimization," *IEEE Transactions on Wireless Communications*, vol. 17, no. 8, pp. 5092–5106, Aug 2018.
- [16] N. Zhao, F. Cheng, F. R. Yu, J. Tang, Y. Chen, G. Gui, and H. Sari, "Caching UAV assisted secure transmission in hyperdense networks based on interference alignment," *IEEE Transactions on Communications*, vol. 66, no. 5, pp. 2281–2294, 2018.
- [17] M. Mozaffari, W. Saad, M. Bennis, and M. Debbah, "Unmanned aerial vehicle with underlaid device-to-device communications: Performance and tradeoffs," *IEEE Transactions on Wireless Communications*, vol. 15, no. 6, pp. 3949–3963, 2016.
- [18] A. Al-Hourani, S. Kandeepan, and S. Lardner, "Optimal LAP altitude for maximum coverage," *IEEE Wireless Commun. Lett.*, vol. 3, no. 6, pp. 569–572, Dec. 2014.
- [19] H. He, S. Zhang, Y. Zeng, and R. Zhang, "Joint altitude and beamwidth optimization for UAV-enabled multiuser communications," *IEEE Commun. Lett.*, vol. 22, no. 2, pp. 344–347, Feb. 2018.
- [20] Y. Zeng and R. Zhang, "Energy-efficient UAV communication with trajectory optimization," *IEEE Transactions on Wireless Communications*, vol. 16, no. 6, pp. 3747–3760, June 2017.
- [21] Q. Wu, Y. Zeng, and R. Zhang, "Joint trajectory and communication design for multi-UAV enabled wireless networks," *IEEE Transactions on Wireless Communications*, vol. 17, no. 3, pp. 2109–2121, March 2018.
- [22] Z. Yang, C. Pan, K. Wang, and M. Shikh-Bahaei, "Energy efficient resource allocation in UAV-enabled mobile edge computing networks," *IEEE Transactions on Wireless Communications*, vol. 18, no. 9, p. 4576–4589, Sep 2019. [Online]. Available: <http://dx.doi.org/10.1109/twc.2019.2927313>

- [23] Y. Mao, C. You, J. Zhang, K. Huang, and K. B. Letaief, "A survey on mobile edge computing: The communication perspective," *IEEE Communications Surveys & Tutorials*, vol. 19, no. 4, pp. 2322–2358, 2017.
- [24] C. Wang, C. Liang, F. R. Yu, Q. Chen, and L. Tang, "Computation offloading and resource allocation in wireless cellular networks with mobile edge computing," *IEEE Transactions on Wireless Communications*, vol. 16, no. 8, pp. 4924–4938, Aug 2017.
- [25] W. Zhang, Y. Wen, K. Guan, D. Kilper, H. Luo, and D. O. Wu, "Energy-optimal mobile cloud computing under stochastic wireless channel," *IEEE Transactions on Wireless Communications*, vol. 12, no. 9, pp. 4569–4581, Sep. 2013.
- [26] S. Jeong, O. Simeone, and J. Kang, "Mobile edge computing via a UAV-mounted cloudlet: Optimization of bit allocation and path planning," *IEEE Transactions on Vehicular Technology*, vol. 67, no. 3, pp. 2049–2063, March 2018.
- [27] Y. Du, K. Yang, K. Wang, G. Zhang, Y. Zhao, and D. Chen, "Joint resources and workflow scheduling in uav-enabled wirelessly-powered mec for iot systems," *IEEE Transactions on Vehicular Technology*, pp. 1–14, 2019.
- [28] V. Mnih *et al.*, "Human-level control through deep reinforcement learning," *Nature*, vol. 518, no. 7540, p. 529–533, Feb. 2015.
- [29] H. van Hasselt, A. Guez, and D. Silver, "Deep reinforcement learning with double Q-learning," 2015.
- [30] T. P. Lillicrap, J. J. Hunt, A. Pritzel, N. Heess, T. Erez, Y. Tassa, D. Silver, and D. Wierstra, "Continuous control with deep reinforcement learning," *arXiv preprint arXiv:1509.02971*, 2015.
- [31] T. Schaul, J. Quan, I. Antonoglou, and D. Silver, "Prioritized experience replay," *arXiv preprint arXiv:1511.05952*, Nov. 2015.
- [32] X. Wang, K. Wang, S. Wu, S. Di, H. Jin, K. Yang, and S. Ou, "Dynamic Resource Scheduling in Mobile Edge Cloud with Cloud Radio Access Network," *IEEE Trans. Parallel Distrib. Syst.*, vol. 29, no. 11, pp. 2429–2445, Nov. 2018.
- [33] S. Mitchell, M. G. O. Sullivan, and I. Dunning, "Pulp : A linear programming toolkit for python," in *Python*, 2011.
- [34] S. Diamond and S. Boyd, "CVXPY: A Python-embedded modeling language for convex optimization," *Journal of Machine Learning Research*, vol. 17, no. 83, pp. 1–5, 2016.
- [35] V. R. Konda and J. N. Tsitsiklis, "Actor-critic algorithms," in *Advances in neural information processing systems*, 2000, pp. 1008–1014.
- [36] H. Van Hasselt, A. Guez, and D. Silver, "Deep reinforcement learning with double Q-learning," in *Thirtieth AAAI Conference on Artificial Intelligence*, Mar. 2016.
- [37] C. J. Watkins and P. Dayan, "Q-learning," *Machine learning*, vol. 8, no. 3-4, pp. 279–292, 1992.
- [38] J. Hamari, J. Koivisto, H. Sarsa *et al.*, "Does gamification work?-a literature review of empirical studies on gamification." in *HICSS*, vol. 14, no. 2014, 2014, pp. 3025–3034.
- [39] A. R. Mahmood, H. P. Van Hasselt, and R. S. Sutton, "Weighted importance sampling for off-policy learning with linear function approximation," in *Advances in Neural Information Processing Systems*, 2014, pp. 3014–3022.